

## Adaptive Model-Based Mammogram Enhancement

Michal Haindl\*    Václav Remeš \*<sup>†</sup>  
*Institute of Information Theory and Automation\**  
*Academy of Sciences of the Czech Republic*  
*and*  
*Faculty of Information Technology<sup>†</sup>*  
*Czech Technical University in Prague*  
*Prague, Czech Republic*  
*Email: {haindl, remes}@utia.cas.cz*

**Abstract**—Five fully automatic methods for X-ray digital mammogram enhancement based on a fast analytical textural model are presented. These efficient single and double view enhancement methods are based on the underlying two-dimensional adaptive causal autoregressive texture model. The methods locally predict breast tissue texture from single or double view mammograms and enhance breast tissue abnormalities, such as the sign of a developing cancer, using the estimated model prediction statistics. The double-view mammogram enhancement is based on the cross-prediction of two mutually registered left and right breasts mammograms or alternatively a temporal sequence of mammograms. The single-view mammogram enhancement is based on modeling prediction error in case of not the both breasts' mammograms being available.

**Keywords**—mammography; image enhancement; MRF; textural models;

### I. INTRODUCTION

Breast cancer is the most common type of cancer among middle-aged women in most developed countries [1], [2]. Almost one woman in ten grows a breast cancer in her life. To lower the mortality rate, women in the developed countries usually regularly attend a preventive mammography screening. However, around 25% of radiologically visible cancers are missed by the radiologists at screening [3]. This means that millions of cancer cases are missed and therefore even a slightest improvement in the detection methods could have a huge impact and save many lives.

The biggest problem with current CAD (computer-aided diagnosis) systems is their large false negative rate and an even larger false positive rate. Most CAD systems (e.g., [1], [4]) point out 2-3 regions of interest (ROIs) per mammogram on average. Taking into account that there are about 8 malignant mammograms in 1000 [3], the radiologists consider the current CAD systems as misleading.

An alternative way is to automatically enhance mammograms to support radiologists with their visual mammogram evaluation. Several mammogram enhancement methods have been published [5], [6], [7], [8], [9], [10], [11], [12], [13], [14], [15], [16], [17]. Salvado and Roque [9] use wavelet analysis to detect microcalcifications, Dippel et al. [7] compare the merits of using either Laplacian pyramids or wavelet analysis for whole mammogram enhancement, Sakellaropoulos et al. [8] designed an adaptive

wavelet based method for enhancing the contrast of the whole mammograms. Pisano et al. [6] and Rahmati et al. [15] use contrast-limited adaptive histogram equalization techniques to reduce noise and enhance mammograms. This approach based on the local windows histogram equalization can provide subtle edge information but might degrade performance in the screening setting by enhancing the visibility of nuisance information [6]. The [15] method requires interactive placement of the seed point. Mencattini et al. [12] selectively enhance segmented mammograms regions using wavelet transformation. Wang et al. published [17] enhancement method based on the idea of image matting. This method has promising results (Fig. 5) but needs a lot of time to compute (tens of minutes for 2Mpix images on a regular PC). A nonlinear unsharp masking combined with nonlinear filtering for mammogram enhancement was introduced by Panetta et al. [16]. Tang et al. [14] use local contrast enhancement in the wavelet domain.

An approach to diagnostic evaluation of screening mammograms based on local statistical Gaussian mixture textural models was proposed in [13]. The local evaluation tool has the form of a multivariate probability density of gray levels in a suitably chosen search window. First, the density function in the form of Gaussian mixture is estimated from data obtained by scanning the mammogram with the search window. The estimated mixture was evaluated at each position and displays the corresponding log-likelihood value as a gray level at the window center. The resulting log-likelihood image closely correlates with the structural details of the original mammogram and emphasizes unusual places, but the method is very computationally demanding.

Radiologists regularly compare the bilateral mammogram pairs during mammogram screening in search for breast abnormalities. The mutual mammograms enhancement requires accurate registration of both breast X-ray images, which is difficult due to their elasticity. Marias et al. [18], [19] use thin-plate spline transformation [20] to align the breasts and then use wavelet based feature detection to find internal landmarks. Thin-plate spline based approach is also used by Wirth et al. in [21]. Hachama [22] deals only with the comparison of temporal mammograms based on a general method for registering images with

the presence of abnormalities. However, it needs the prior abnormalities distribution knowledge. The registration and transformation are based on the Bayesian maximum a posteriori probability approach and minimization of the registration and deformation energy.

The novelty of the presented methods is that whereas other alternative methods usually use simple pixel difference or trivial statistics like cross-correlation to compare the left and right images, we use the mammograms of one breast as a learning sample for the 2DCAR breast texture model [23], [24] and then try to analyze the other mammogram based on this acquired information. Using the 2DCAR model for bilateral comparison, we achieve a result which is robust to inaccurate registration, very fast, and which gives improved enhancement results than just a single-view analysis even using similar local texture modeling.

## II. MAMMOGRAM ENHANCEMENT

Our methods presume that left and right breasts are architecturally symmetrical. This presumption is indeed reasonable, since radiologists frequently compare double-view mammograms to find asymmetrical parts, which could indicate a developing cancer. The texture based symmetry detection neither needs to assume the pixel-wise correspondence of the both breast images, nor their ideal sub-pixel registration inside the breast area.

The presented enhancement methods (7)-(9),(12),(13) consist of three major steps: registration, model parameters adaptive estimation, and the cross-prediction based analysis.

### A. Mammogram Registration

The registration process is described for mammographic MLO views (medio-lateral oblique), but it can be easily adapted also for CC views (cranio-caudal). Since we compare the images based on textural features rather than pixel-wise, we do not require as precise registration as other methods, and can use a simple registration based on the affine transformation.

Three reference points are needed for the affine transformation. We chose the nipple and one point above and one below it which are closest to the pectoral muscle.

The nipple is located using the heuristic method described in [25]. It works on the idea of the nipple being a point on the skin-line of the breast which is the most distant from the line of the pectoral muscle. After the candidates for the nipple reference points have been found in both the mammograms, the positions of the reference points can still slightly differ in both images. Therefore, we adjust their position by searching the neighborhood on the skin line of the breast for the most correlated window.

The remaining reference point candidates have to be further adjusted as well. Since the bilateral mammograms usually do not cover the same area of the breast, some anatomical parts of the breast can be seen only in one of the images and therefore the reference points wouldn't match. To make up for this problem, we measure the

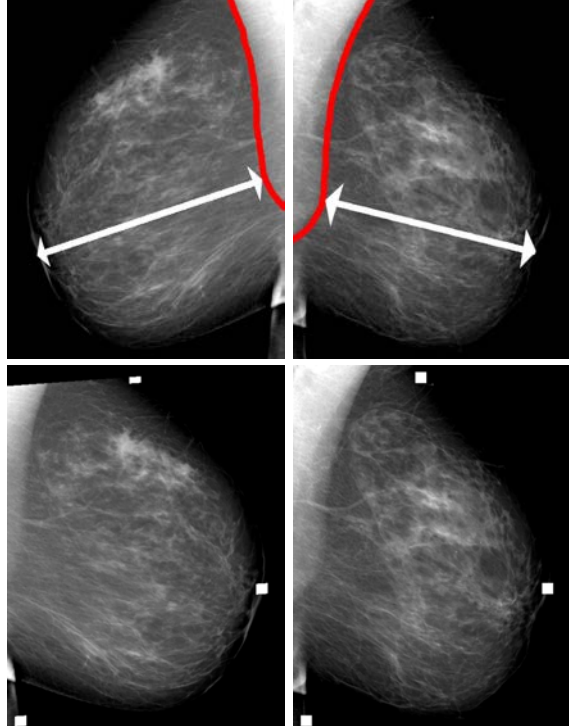


Figure 1. Registered mammograms with visible reference points.

distance of the points to the nipple, weighted by the nipples distance to the pectoral muscle. The weighting compensates for the differences of positioning of the breast in the mammogram which could result in one image displaying the breast bigger than the other one. We then adjust the corresponding reference points, so that they are on the skin line with the most similar weighted distance to the nipple possible.

Having found the reference points, the affine transformation is performed. Fig.1 in the upper row shows the images of right and left breast with marked line of the pectoral muscle (colored in red) and the distance from the pectoral muscle to the nipple. The lower row shows the registered breasts with the reference points painted as white squares with the right breast (shown on the left side) transformed to match the left breast.

### B. Adaptive Textural Model

The X-ray mammographic tissue is locally modeled by its dedicated independent Gaussian noise-driven autoregressive random field two-dimensional texture model (2DCAR), which is a rare exception among Markovian random field model family that can be completely analytically solved [26], [27]. Apart from that, this descriptive model has good modeling performance, all statistics can be evaluated recursively, and the model is very fast to evaluate. The 2DCAR random field is a Markovian family of random variables with a joint probability density on the set of all possible realizations  $Y$  of the  $M \times N$  lattice  $I$ , subject to the following condition:

$$p(Y | \gamma, \sigma^{-2}) = (2\pi\sigma^2)^{-\frac{(MN-1)}{2}} \exp \left\{ \frac{-1}{2} \text{tr} \left\{ \sigma^{-2} \begin{pmatrix} -\alpha \\ \gamma^T \end{pmatrix}^T \tilde{V}_{MN-1} \begin{pmatrix} -\alpha \\ \gamma^T \end{pmatrix} \right\} \right\},$$

where  $\alpha$  is a unit vector,  $\text{tr}()$  is a trace of the corresponding matrix, and the following notation is used

$$\begin{aligned} \tilde{V}_{r-1} &= \sum_{k=1}^{r-1} \begin{pmatrix} Y_k Y_k^T & Y_k X_k^T \\ X_k Y_k^T & X_k X_k^T \end{pmatrix} \\ &= \begin{pmatrix} \tilde{V}_{y(r-1)} & \tilde{V}_{xy(r-1)}^T \\ \tilde{V}_{xy(r-1)} & \tilde{V}_{x(r-1)} \end{pmatrix}. \end{aligned}$$

Here,  $r = [r_1, r_2, \phi]$  is a spatial multiindex denoting history of movements on the rectangular lattice  $I$ , where  $r_1, r_2$  are row and column indices, and  $\phi \in \{0^\circ, 45^\circ, 90^\circ, 135^\circ, 180^\circ, 225^\circ, 270^\circ, 315^\circ\}$  is the direction of the model development. The contextual neighborhood weights and the additive noise variance  $\gamma, \sigma^2$  are unknown model parameters to be estimated. The 2DCAR model can be expressed as a stationary causal uncorrelated noise-driven 2D autoregressive process:

$$Y_r = \gamma_\phi X_r + e_r, \quad (1)$$

where  $\gamma_\phi = [a_1, \dots, a_\eta]$  is the parameter vector,  $\eta = \text{cardinality}(I_r^c)$ ,  $I_r^c$  denotes a causal (or alternatively unilateral) contextual neighborhood (i.e., all support pixels were previously visited and thus they are known). Furthermore,  $e_r$  denotes white Gaussian noise with zero mean and a constant but unknown variance  $\sigma^2$ , and  $X_r$  is a support vector of  $Y_{r-s}$  where  $s \in I_r^c$ . The method uses a locally adaptive version of this 2DCAR model [27], where its recursive statistics are modified by an exponential forgetting factor, i.e., a constant smaller than 1 which is used to weight the older data.

*Parameter Estimation:* Parameter estimation of a 2DCAR model using either the maximum likelihood, or the least square or Bayesian methods can be found analytically. The Bayesian parameter estimates of the 2DCAR model using the normal-gamma parameter prior are:

$$\hat{\gamma}_{r-1}^T = V_{x(r-1)}^{-1} V_{xy(r-1)}, \quad (2)$$

$$\hat{\sigma}_{r-1}^2 = \frac{\lambda(r-1)}{\beta(r)}, \quad (3)$$

where

$$\begin{aligned} \lambda(r-1) &= V_{y(r-1)} - V_{xy(r-1)}^T V_{x(r-1)}^{-1} V_{xy(r-1)}, \\ V_{(r-1)} &= \tilde{V}_{(r-1)} + V_{(0)}, \\ \beta(r) &= \beta(0) + r - 1, \end{aligned}$$

and  $\beta(0)$  is an initialization constant and submatrices in  $V_{(0)}$  are from the parameter prior. The parameter estimates (2),(3) can also be evaluated recursively [27]. The posterior probability density [27] of the model is:

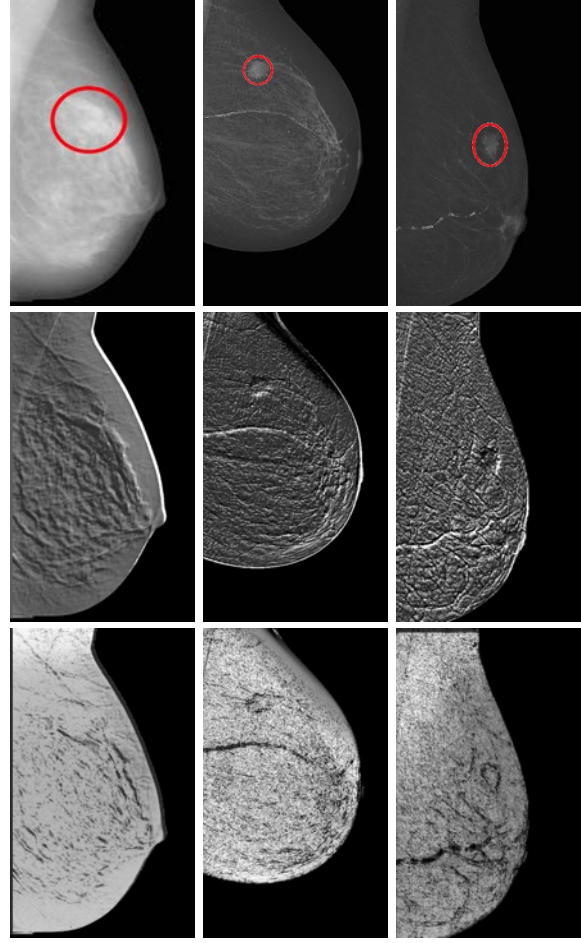


Figure 2. Three different malignant breast images (single view analysis) - leftmost is from the DDSM database, the other two are from the INbreast. Upper row shows original images with the ground truth, middle row shows the modelled predicted gradient and bottom row shows prediction probability densities.

$$p(Y_r | Y^{(r-1)}, \hat{\gamma}_{r-1}) = \frac{\Gamma(\frac{\beta(r)-\eta+3}{2})}{\Gamma(\frac{\beta(r)-\eta+2}{2}) \pi^{\frac{1}{2}} (1 + X_r^T V_{x(r-1)}^{-1} X_r)^{\frac{1}{2}} |\lambda(r-1)|^{\frac{1}{2}}} \left( 1 + \frac{(Y_r - \hat{\gamma}_{r-1} X_r)^T \lambda_{(r-1)}^{-1} (Y_r - \hat{\gamma}_{r-1} X_r)}{1 + X_r^T V_{x(r-1)}^{-1} X_r} \right)^{-\frac{\beta(r)-\eta+3}{2}} \quad (4)$$

And the conditional mean value predictor of the one-step-ahead predictive posterior density (4) for the normal-gamma parameter prior is

$$E \{ Y_r | Y^{(r-1)} \} = \hat{\gamma}_{r-1} X_r. \quad (5)$$

*Prediction:* The conditional mean value of the one-step-ahead predictive posterior density for the normal-gamma parameter prior is

$$E \left\{ Y_r | Y^{(r-1)} \right\} = \hat{\gamma}_{r-1} X_r . \quad (6)$$

The predictor (6) is used only for single-view mammogram enhancement. For double-view mammograms where there are available both left and right breasts mammograms the method uses the cross-prediction (10),(11).

### C. Enhancement Methods

Let us denote two mutually registered (e.g., left and right breasts' mammograms)  $Y$  and  $\tilde{Y}$ , the local 2DCAR model parameters estimates (2), (3) computed on the mammogram image  $Y$   $\hat{\gamma}_{r-1}^T, \hat{\sigma}_{r-1}^2$ . The same parameter estimates (2), (3) computed on the other mammogram  $\tilde{Y}$  are denoted  $\tilde{\gamma}_{r-1}^T, \tilde{\sigma}_{r-1}^2$ , and the corresponding support vector is  $\tilde{X}_r$ . The directional models are computed in the following angles  $\phi \in \Phi = \{0^\circ, 45^\circ, 90^\circ, 135^\circ, 180^\circ, 225^\circ, 270^\circ, 315^\circ\}$ . The proposed single and double view enhancement methods use all eight possible directional prediction or cross-prediction error statistics. However any fewer number of directional models can be used if needed. For example, in case of real time enhancement directly during a digital mammogram scanning.

*Single-View Enhancement:* The single-view enhancement the multidirectional prediction error (7), the multidirectional prediction probability (8), and the multidirectional absolute prediction error (9) methods are computed from up to eight directional models, i.e.,

$$Y_r^{enh1} = \sum_{\forall \phi \in \bar{\Phi}} (Y_{r+1} - \hat{\gamma}_{r-1} X_r) , \quad (7)$$

$$Y_r^{enh2} = \sum_{\forall \phi \in \bar{\Phi}} p(Y_r | Y^{(r-1)}, \hat{\gamma}_{r-1}) , \quad (8)$$

$$Y_r^{enh3} = \sum_{\forall \phi \in \bar{\Phi}} |Y_{r+1} - \hat{\gamma}_{r-1} X_r| , \quad (9)$$

where  $\bar{\Phi} \subseteq \Phi$ . All the enhanced values are normalized into the 0 – 255 range.

*Double-View Enhancement:* The double-view enhancement is based on statistics computed on one breast image and applied to the complementary one. The cross-prediction between images  $Y, \tilde{Y}$  is computed as follows:

$$E \left\{ \tilde{Y}_r | Y^{(r-1)} \right\} = \hat{\gamma}_{r-1} \tilde{X}_r \quad (10)$$

and the opposite direction cross-prediction is analogously

$$E \left\{ Y_r | \tilde{Y}^{(r-1)} \right\} = \tilde{\gamma}_{r-1} X_r . \quad (11)$$

The enhanced mammograms are then the corresponding cross-prediction statistics images. The corresponding cross-prediction probability densities are  $p(\tilde{Y}_r | \tilde{Y}^{(r-1)}, \hat{\gamma}_{r-1})$  and  $p(Y_r | Y^{(r-1)}, \tilde{\gamma}_{r-1})$ .

The proposed double-view enhancement methods the multidirectional cross-prediction error (12) and the multidirectional cross-prediction probability (13) are

$$Y_r^{com1} = \sum_{\forall \phi \in \bar{\Phi}} \left( \tilde{Y}_{r+1} - \hat{\gamma}_{r-1} X_r \right) , \quad (12)$$

$$Y_r^{com2} = \sum_{\forall \phi \in \bar{\Phi}} p(\tilde{Y}_r | \tilde{Y}^{(r-1)}, \hat{\gamma}_{r-1}) . \quad (13)$$

## III. EXPERIMENTAL RESULTS

The algorithm was tested on mammograms from the INbreast database [28] and the Digital Database for Screening Mammography (DDSM) from the University of South Florida [29]. The DDSM database contains 2620 four view (left and right cranio-caudal (LCC, RCC) and medio-lateral oblique (LMLO, RMLO)) mammograms in different resolutions digitized from original X-ray films. Single mammogram cases are divided into normal, benign, benign without callback volumes and cancer.

The INbreast database is a mammographic database, with images acquired at a Breast Centre, located in a University Hospital (Hospital de São João, Breast Centre, Porto, Portugal). INbreast has a total of 115 cases (410 images) of which 90 cases are from women with both breasts (4 images per case) and 25 cases are from mastectomy patients (2 images per case). Several types of lesions (masses, calcifications, asymmetries, and distortions) are included. Accurate contours made by specialists are also provided in XML format.

Fig.2 shows three single-view MLO mammogram enhancements from the DDSM and INbreast databases using one directional diagonal 2DCAR model moving from the bottom right to the top left.

The single-view enhancement method is compared with three different state-of-the-art methods: a nonlinear unsharp masking based method by Panetta et al. [16], a wavelet decomposition based method by Tang et al. [14] and a matting based method by Wang et al. [17] (Fig.5). Compared with our results, these methods tend to highlight mostly the brighter areas of the images while not taking into account the local texture. While the method by Wang et al. [17] gives comparable results, it takes distinctively longer to compute compared to our method - tens of minutes whereas our method needs just several seconds.

Double-view medio-lateral oblique (Figs.3,4) digital mammograms' enhancements from the INbreast database show the cross-prediction based enhancement performance. Comparing the cross-prediction enhancements on Fig.3 with the same breast single-view enhancement on Fig.2, the benefits of the cross-prediction are clearly visible.

Our double-view enhancement method is compared with the registered image pixel difference which is standardly used for comparison ([18], [21], [22])

$$\Delta Y_r = \max\{Y_r^R - Y_r^L, 0\} . \quad (14)$$

This standard double-view enhancement method (Figs.3,4 - second columns) is inferior compared to the both

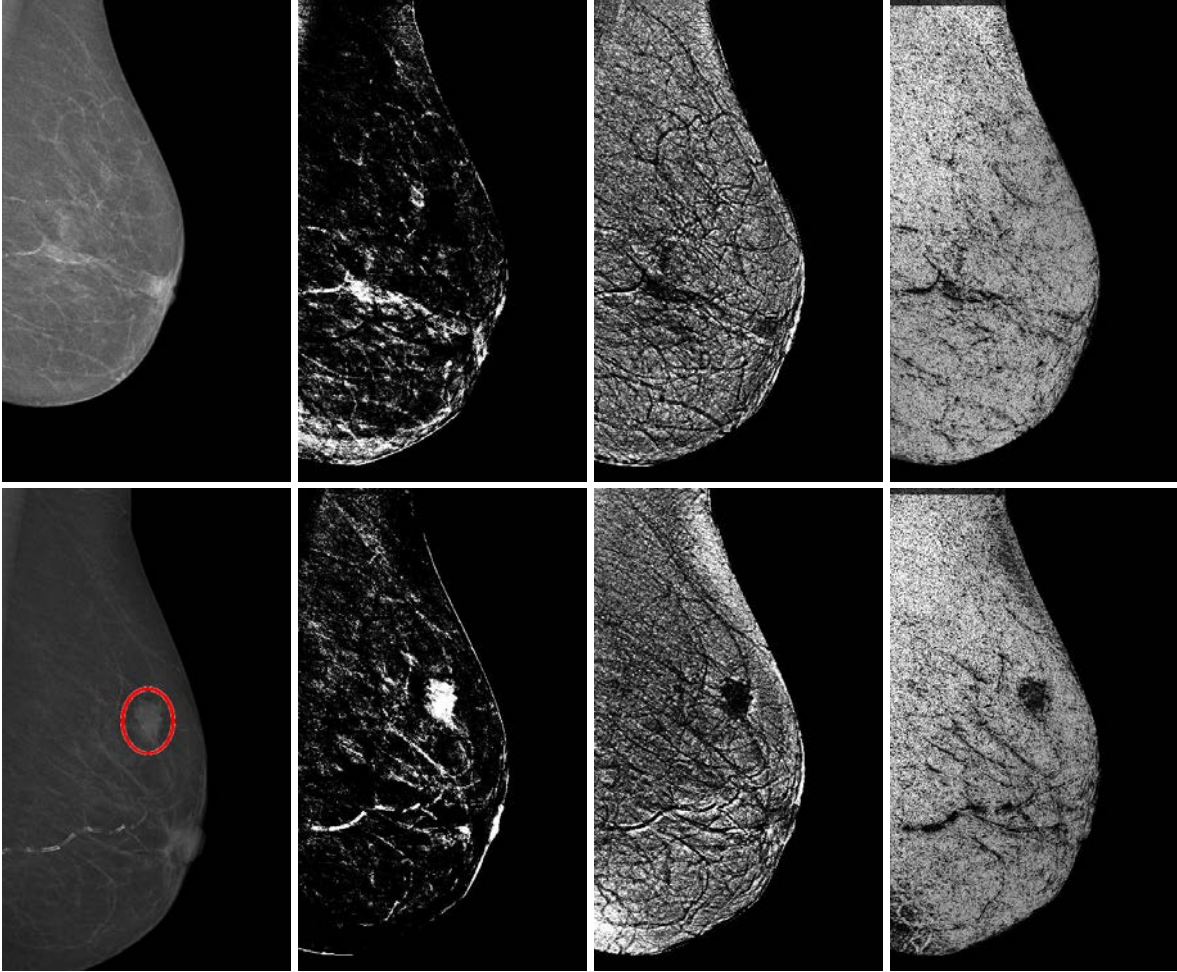


Figure 3. Multiple-view medio-lateral mammogram enhancement consecutively rightwards - ground truth, pixel difference between registered LMLO and RMLO, cross-predicted gradient, and cross-prediction probability density. The upper row contains LMLO, bottom row RMLO.

proposed double-view enhancement methods ((12), (13)) which simultaneously exhibit more contrast and increased details' visibility. All five proposed enhancement methods are very fast, they can be computed on the presented mammograms with a standard PC in a matter of several seconds.

#### IV. CONCLUSION

We proposed five novel fast methods for completely automatic mammogram enhancement which highlight regions of interest, detected as textural abnormalities and simultaneously decrease the additive measurement noise. Cancerous areas typically manifest themselves in X-ray mammography as such textural defects. Thus the enhanced mammograms can help radiologists to decrease their false negative evaluation rate. These methods are based on the underlying two-dimensional adaptive CAR texture model. Although the algorithms use random field type model, the model is very fast due to efficient recursive model predictor estimation and therefore is much

faster than the usual alternative Markov chain Monte Carlo estimation approach. The enhancement can be either single or double view depending on the data available. The single-view methods allow significant mammogram enhancement without the need of paired mammogram registration. The double-view methods benefit from mutual textural information in the registered bilateral breast pairs. Contrary to the simple pixel difference values or cross-correlations, the textural feature comparison brings increased robustness to registration inaccuracies inevitably encountered due to the elasticity of the breast. The double-view methods could alternatively be used for the enhancement of a temporal sequence of mammograms.

#### ACKNOWLEDGEMENTS

This research was supported by grant GAČR 14-10911S

#### REFERENCES

- [1] T. Tweed and S. Miguet, "Automatic detection of regions of interest in mammographies based on a combined analysis of texture and histogram," in *Pattern Recognition*, 2002.

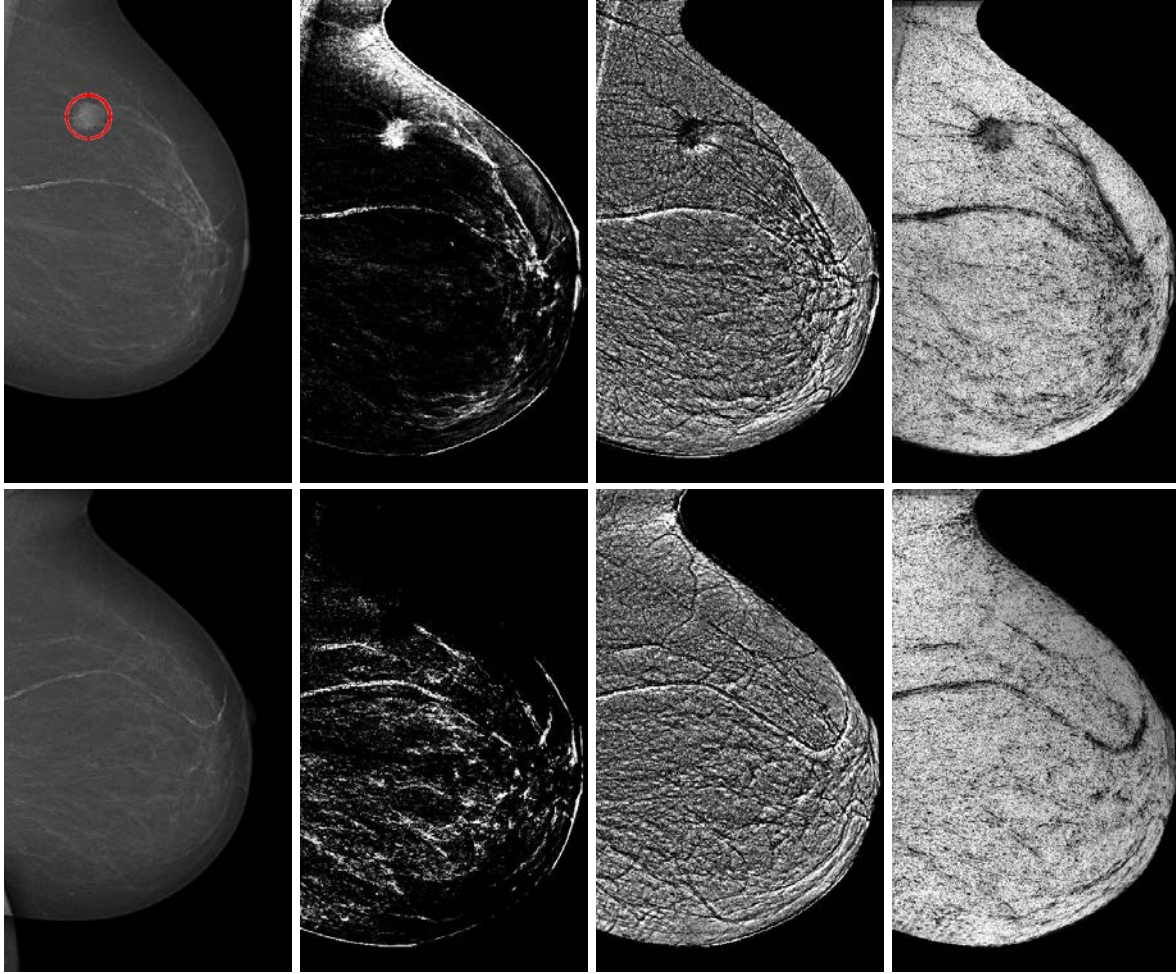


Figure 4. Multiple-view medio-lateral mammogram enhancement consecutively rightwards - ground truth, pixel difference between registered LMLO and RMLO, cross-predicted gradient, and cross-prediction probability density. The upper row contains LMLO, bottom row RMLO.

- Proceedings, 16th International Conference on*, vol. 2. Los Alamitos, CA, USA: IEEE Computer Society, 2002, pp. 448–452.
- [2] H. Qi and N. A. Diakides, “Thermal infrared imaging in early breast cancer detection - a survey of recent research,” in *Proceedings of the 25th Annual International Conference of the IEEE Engineering in Medicine and Biology Society*, vol. 2. IEEE, 2003, pp. 1109–1112.
- [3] Taylor, P. and Champness, J. and Given-Wilson, R. and Johnston, K. and Potts, H., “Impact of computer-aided detection prompts on the sensitivity and specificity of screening mammography,” *Health Technology Assessment*, vol. 9, no. 6, 2005.
- [4] M. Haindl, S. Mikeš, and G. Scarpa, “Unsupervised detection of mammogram regions of interest,” in *Knowledge-Based Intelligent Information and Engineering Systems*, ser. LNAI, B. Apolloni, R. J. Howlett, and L. Jain, Eds., vol. 4694. Springer, 2007, pp. 33–40.
- [5] C.-M. Chang and A. Laine, “Coherence of multiscale features for enhancement of digital mammograms,” *IEEE Transactions on Information Technology in Biomedicine*, vol. 3, no. 1, pp. 32–46, 1999.
- [6] E. D. Pisano, E. B. Cole, B. M. Hemminger, M. J. Yaffe, S. R. Aylward, A. D. Maidment, R. E. Johnston, M. B. Williams, L. T. Niklason, E. F. Conant *et al.*, “Image processing algorithms for digital mammography: A pictorial essay,” *Radiographics*, vol. 20, no. 5, pp. 1479–1491, 2000.
- [7] S. Dippel, M. Stahl, R. Wiemker, and T. Blaffert, “Multiscale contrast enhancement for radiographies: Laplacian pyramid versus fast wavelet transform,” *Medical Imaging, IEEE Transactions on*, vol. 21, no. 4, pp. 343–353, 2002.
- [8] P. Sakellaropoulos, L. Costaridou, and G. Panayiotakis, “A wavelet-based spatially adaptive method for mammographic contrast enhancement,” *Physics in medicine and biology*, vol. 48, no. 6, p. 787, 2003.
- [9] J. Salvado and B. Roque, “Detection of calcifications in digital mammograms using wavelet analysis and contrast enhancement,” in *Intelligent Signal Processing, 2005 IEEE International Workshop on*. IEEE, 2005, pp. 200–205.

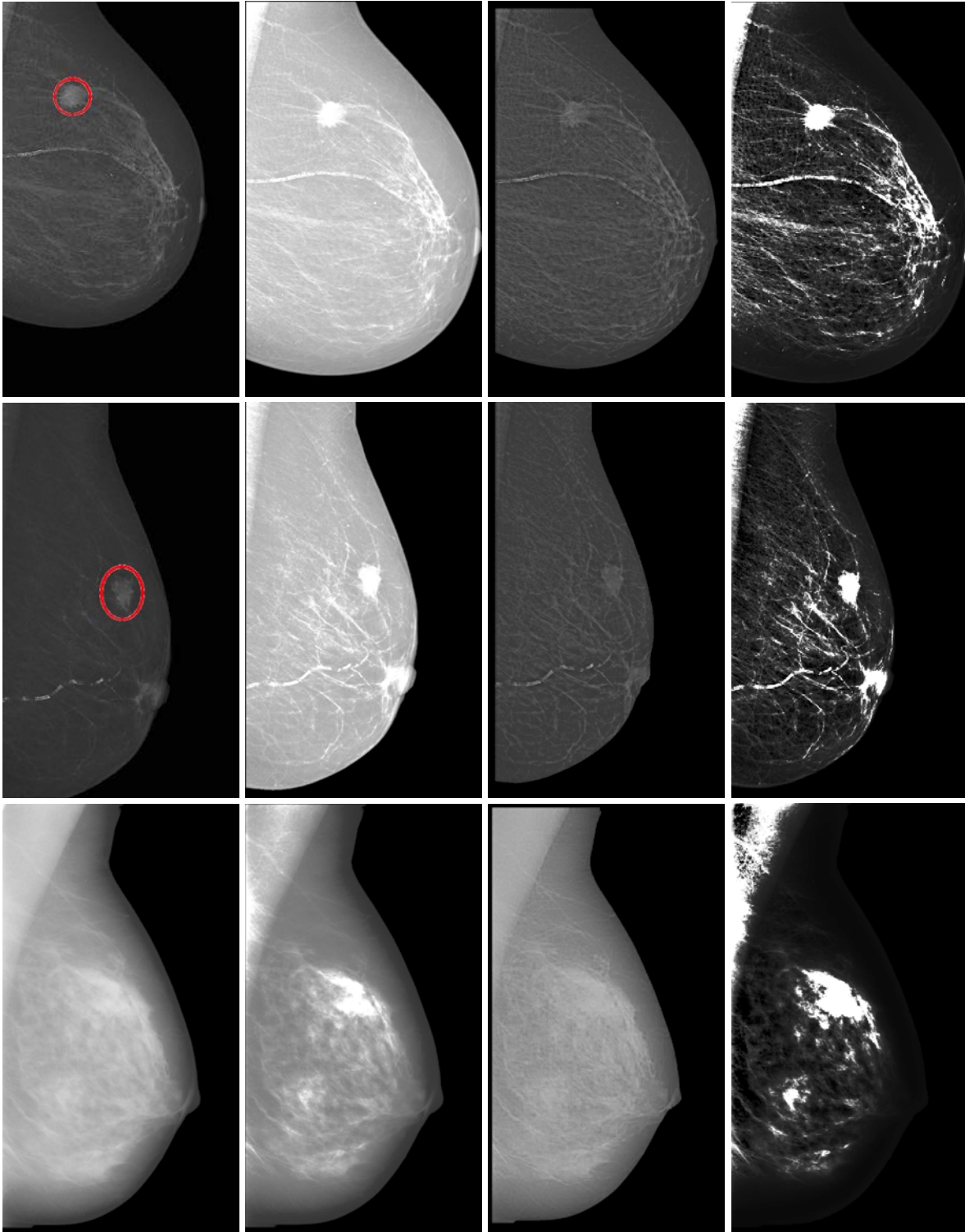


Figure 5. Three methods from different authors for comparison. Left to right: original image, method by Panetta et al. [16], wavelet decomposition based method by Tang et al. [14] and a matting based method by Wang et al. [17].

- [10] Z. Yan, Y. Zhang, B. Liu, J. Zheng, L. Lu, Y. Xie, Z. Liang, and J. Li, "Extracting hidden visual information from mammography images using conjugate image enhancement software," in *Information Acquisition, 2005 IEEE International Conference on*, IEEE Engineering in Medicine and Biology Society. IEEE, Aug. 2005, pp. 4775 – 4778.
- [11] K. Thangavel, M. Karnan, R. Sivakumar, and A. Mohideen, "Cad system for preprocessing and enhancement of digital mammograms," *Graphics, Vision and Image Processing*, pp. 55–60, 2007. [Online]. Available: <http://www.icgst.com/gvip/v7/P1150527002.html>
- [12] A. Mencattini, M. Salmeri, R. Lojacono, M. Frigerio, and F. Caselli, "Mammographic images enhancement and denoising for breast cancer detection using dyadic wavelet processing," *Instrumentation and Measurement, IEEE Transactions on*, vol. 57, no. 7, pp. 1422–1430, 2008.
- [13] J. Grim, P. Somol, M. Haindl, and J. Daneš, "Computer-aided evaluation of screening mammograms based on local texture models," *IEEE Transactions on Image Processing*, vol. 18, no. 4, pp. 765 – 773, 2009.
- [14] J. Tang, X. Liu, and Q. Sun, "A direct image contrast enhancement algorithm in the wavelet domain for screening mammograms," *Selected Topics in Signal Processing, IEEE Journal of*, vol. 3, no. 1, pp. 74–80, 2009.
- [15] P. Rahmati, G. Hamarneh, D. Nussbaum, and A. Adler, "A new preprocessing filter for digital mammograms," in *Image and Signal Processing*. Springer, 2010, pp. 585–592.
- [16] K. Panetta, Y. Zhou, S. Agaian, and H. Jia, "Nonlinear unsharp masking for mammogram enhancement," *Information Technology in Biomedicine, IEEE Transactions on*, vol. 15, no. 6, pp. 918–928, 2011.
- [17] H. Wang, J.-B. Li, L. Wu, and H. Gao, "Mammography visual enhancement in cad-based breast cancer diagnosis," *Clinical imaging*, vol. 37, no. 2, pp. 273–282, 2013.
- [18] K. Marias, C. P. Behrenbruch, M. Brady, S. Parbhoo, and A. Seifalian, "Multi-scale landmark selection for improved registration of temporal mammograms," in *International Workshop on Database Machines*, 2000.
- [19] Marias, K. and Behrenbruch, C. and Parbhoo, S. and Seifalian, A. and Brady, M., "A registration framework for the comparison of mammogram sequences," *Medical Imaging, IEEE Transactions on*, vol. 24, no. 6, pp. 782–790, June 2005.
- [20] Harder, R L and Desmarais, R N, "Interpolation using surface splines." *Journal of Aircraft*, vol. 9, no. 2, pp. 189–191, 1972. [Online]. Available: <http://www.mendeley.com/research/interpolation-using-surface-splines-1/>
- [21] M. A. Wirth, J. Narhan, and D. Gray, "A model for nonrigid mammogram registration using mutual information," in *In International Workshop on Digital Mammography*, 2002.
- [22] Hachama, M. and Richard, F. and Desolneux, A., "A mammogram registration technique dealing with outliers," in *Biomedical Imaging: Nano to Macro, 2006. 3rd IEEE International Symposium on*, April 2006, pp. 458–461.
- [23] M. Haindl and V. Havlíček, "A multiscale colour texture model," in *Pattern Recognition, 2002. Proceedings. 16th International Conference on*, vol. 1. IEEE, 2002, pp. 255–258.
- [24] M. Haindl and S. Šimberová, "A multispectral image line reconstruction method," *Theory & Applications of Image Analysis*, pp. 306–315, 1992.
- [25] F. Georgsson and C. Olsn, "The accuracy of geometric approximation of the mamilla in mammograms," in *CARS'03*, 2003, pp. 956–961.
- [26] M. Haindl, "Texture synthesis," *CWI Quarterly*, vol. 4, no. 4, pp. 305–331, December 1991.
- [27] —, "Visual data recognition and modeling based on local markovian models," in *Mathematical Methods for Signal and Image Analysis and Representation*, ser. Computational Imaging and Vision, L. Florack, R. Duits, G. Jongbloed, M.-C. Lieshout, and L. Davies, Eds. Springer London, 2012, vol. 41, ch. 14, pp. 241–259, 10.1007/978-1-4471-2353-8\_14. [Online]. Available: [http://dx.doi.org/10.1007/978-1-4471-2353-8\\_14](http://dx.doi.org/10.1007/978-1-4471-2353-8_14)
- [28] I. C. Moreira, I. Amaral, I. Domingues, A. Cardoso, M. J. Cardoso, and J. S. Cardoso, "Inbreast: toward a full-field digital mammographic database," *Academic radiology*, vol. 19, no. 2, pp. 236–248, 2012.
- [29] M. Heath, K. Bowyer, D. Kopans, R. Moore, and P. Kegelmeyer, "The digital database for screening mammography," in *Proc. of the 5th Int. Workshop on Digital Mammography*. Medical Physics Publishing, June 2000.